AGU ADVANCING EARTH AND SPACE SCIENCE

Geophysical Research Letters®

RESEARCH LETTER
10.1029/2022GL100411

# Detrainment Dominates CCN Concentrations Around Non-Precipitating Convective Clouds Over the Amazon

**Ramon C. Braga[1,2], Daniel Rosenfeld[3], Meinrat O. Andreae[4,5,6], Christopher Pöhlker[2], Ulrich Pöschl[2], Christiane Voigt[7], Bernadett Weinzierl[8], Manfred Wendisch[9], Mira L. Pöhlker[2,9,10], and Daniel Harrison[1]**

[1]National Marine Science Centre, Southern Cross University, Coffs Harbour, NSW, Australia, [2]Multiphase Chemistry Department, Max Planck Institute for Chemistry, Mainz, Germany, [3]Institute of Earth Sciences, The Hebrew University of Jerusalem, Jerusalem, Israel, [4]Biogeochemistry Department, Max Planck Institute for Chemistry, Mainz, Germany, [5]Scripps Institution of Oceanography, University of California San Diego, La Jolla, CA, USA, [6]Department of Geology and Geophysics, King Saud University, Riyadh, Saudi Arabia, [7]German Aerospace Center (DLR), Institute of Atmospheric Physics, Cologne, Germany, [8]Faculty of Physics, Aerosol Physics and Environmental Physics, University of Vienna, Vienna, Austria, [9]Faculty of Physics and Earth Sciences, Leipzig Institute for Meteorology, University Leipzig, Leipzig, Germany, [10]Experimental Aerosol and Cloud Microphysics Department, Leibniz Institute for Tropospheric Research, Leipzig, Germany

**Key Points:**

- Residual particles from the evaporation of non-precipitating droplets of convective clouds dominate the cloud condensation nuclei (CCN) concentrations around clouds
- The CCN enrichment around the clouds diminishes above the height of warm rain initiation
- Drizzle evaporated from rain clouds leads to the formation of larger CCN particles than droplets evaporated from non-precipitating clouds

**Supporting Information:**

Supporting Information may be found in the online version of this article.

**Correspondence to:**

R. C. Braga,
ramon.braga@scu.edu.au

**Citation:**

Braga, R. C., Rosenfeld, D., Andreae, M. O., Pöhlker, C., Pöschl, U., Voigt, C., et al. (2022). Detrainment dominates CCN concentrations around non-precipitating convective clouds over the Amazon. *Geophysical Research Letters*, *49*, e2022GL100411. https://doi.org/10.1029/2022GL100411

Received 26 JUL 2022
Accepted 3 OCT 2022

**Author Contributions:**

**Data curation:** Christopher Pöhlker, Ulrich Pöschl, Bernadett Weinzierl
**Formal analysis:** Christopher Pöhlker, Manfred Wendisch
**Funding acquisition:** Daniel Harrison
**Investigation:** Daniel Rosenfeld, Mira L. Pöhlker
**Methodology:** Daniel Rosenfeld, Mira L. Pöhlker



**Abstract** We investigated the relationship between the number concentration of cloud droplets ($N_d$) in ice-free convective clouds and of particles large enough to act as cloud condensation nuclei (CCN) measured at the lateral boundaries of cloud elements. The data were collected during the ACRIDICON-CHUVA aircraft campaign over the Amazon Basin. The results indicate that the CCN particles at the lateral cloud boundaries are dominated by detrainment from the cloud. The CCN concentrations detrained from non-precipitating convective clouds are smaller compared to below cloud bases. The detrained CCN particles from precipitating cloud volumes have relatively larger sizes, but lower concentrations. Our findings indicate that CCN particles ingested from below cloud bases are activated into cloud droplets, which evaporate at the lateral boundaries and above cloud base and release the CCN again to ambient cloud-free air, after some cloud processing. These results support the hypothesis that the CCN around the cloud are cloud-processed.

**Plain Language Summary** Interactions of aerosol particles with clouds represent a significant uncertainty in estimates of climate change. Properties of aerosol particles control their ability to act as cloud condensation nuclei (CCN). Accounting for CCN concentrations and sizes available through the evaporation of cloud droplets and raindrops is highly complicated and a crucial challenge for cloud modeling purposes. Based on airborne measurements performed with the German High Altitude and Long Range Aircraft aircraft, we describe a conceptual model for aerosol-cloud interaction at the lateral boundaries of Amazonian convective clouds. We show that the CCN particles at the lateral boundaries of non-precipitating convective clouds originate mostly from evaporated cloud droplets. In precipitating clouds, many of the activated CCN merge and scavenged, as indicated by the fewer and larger CCN around the clouds.

## 1. Introduction

The interaction between clouds and surrounding air is an important but insufficiently observed process influencing the formation and development of convective clouds. The mixing of cloudy volumes with the ambient cloud-free air (detrainment) and the entrainment of subsaturated air into convective clouds lead to a decrease of the liquid water content and droplet concentration but leaves the mean droplet diameter essentially unchanged (Beals et al., 2015; Freud et al., 2011; Khain & Pinsky, 2018). The detrainment process is typically observed at the lateral boundaries and convective cloud tops. It promotes a local increase of cloud condensation nuclei (CCN) concentration near the cloud edges due to the release of residual particles from the evaporating cloud droplets (Andreae et al., 2004; Bera et al., 2016; Freud et al., 2011; Gerber et al., 2008). For convective clouds, the mixing is mostly inhomogeneous and takes place when sub-saturated air is entrained from outside the cloud which results in the total evaporation of some drops of all sizes (Pruppacher & Klett, 1997). In this case, the evaporation rate of cloud droplets significantly exceeds the mixing rate of the cloud with ambient air. For homogeneous mixing conditions (often observed in stratus clouds) the cloud droplets experience nearly identical evaporation during the detrainment process to dry air, resulting in partial evaporation of droplets within the cloud layer (Khain &

**Project Administration:** Ulrich Pöschl, Christiane Voigt, Manfred Wendisch, Daniel Harrison
**Resources:** Ulrich Pöschl
**Supervision:** Daniel Rosenfeld, Ulrich Pöschl, Manfred Wendisch, Daniel Harrison
**Validation:** Daniel Rosenfeld, Bernadett Weinzierl, Mira L. Pöhlker
**Writing – review & editing:** Daniel Rosenfeld, Meinrat O. Andreae, Christopher Pöhlker, Ulrich Pöschl, Christiane Voigt, Bernadett Weinzierl, Manfred Wendisch, Mira L. Pöhlker, Daniel Harrison

Pinsky, 2018; Pruppacher & Klett, 1997). The understanding of these mechanisms is crucial for cloud-modeling purposes and the description of radiative forcing due to aerosol-cloud interactions, since the droplet number concentration and liquid water content determines the optical properties and precipitation efficiency of clouds (Kokhanovsky, 2004; Rosenfeld et al., 2008; Twomey, 1974).

In the course of in situ measurements over the Amazon rain forest, Braga et al. (2017a) have observed that the vertical evolution of the cloud droplet effective radius ($r_e$) generally follows that of the calculated adiabatic $r_e$. This pattern was found to be a result of the nearly inhomogeneous mixing behavior of the convective clouds with the ambient air. Such characteristics of turbulent mixing of convective clouds were also observed by Burnet and Brenguier (2007) and Freud et al. (2011). In this study, we investigate how detrainment in convective clouds and the associated cloud droplet evaporation affects the CCN number concentration at the lateral cloud boundaries. Our analysis is based on measurements of $N_d$ and the number concentration of accumulation mode particles ($N_{acc}$; 0.1 μm < diameter <1.0 μm) within and around growing cumuli in the Amazonian dry season in September 2014. By acting as CCN, accumulation mode particles are most important for the formation of natural clouds (Rogers & Yau, 1989). Aerosol particles with diameters less than 0.1 μm and hygroscopicities typical of continental atmospheres may only be activated to form cloud droplets at higher supersaturations than usually occur at cloud bases. Typically, such small CCN particles are activated into cloud droplets at higher levels above cloud bases of warm convective clouds when the coalescence process is intense (Fan et al., 2018). Atmospheric particles larger than 1.0 μm are much fewer in number and therefore contribute little to the total number concentration of cloud droplets. Therefore it is justified to assume $N_{acc}$ as a proxy of CCN number concentrations (Haarig et al., 2019; Mamouri & Ansmann, 2016).

The measurements used in our analysis were collected during the ACRIDICON-CHUVA (Aerosol, Cloud, Precipitation, and Radiation Interactions and Dynamics of Convective Cloud Systems–Cloud Processes of the Main Precipitation Systems in Brazil: A Contribution to Cloud Resolving Modeling and to the Global Precipitation measurements) airborne campaign (Wendisch et al., 2016). The results of this study show a tight relationship between droplet activation efficiency (ratio $N_d/N_{acc}$) and supersaturation over water ($S_w$) for convective clouds over the Amazon. At cloud base, these findings show the expected relationships between aerosol size distribution, critical supersaturation, and $N_d$, since the CCN $S_w$ spectra and updraft speed determines $N_d$ at cloud bases. At higher levels, however, our findings suggest an inverse causality: the evaporation of droplets detrained from non-precipitating cumuli dominates $N_{acc}$ measured around the clouds.

## 2. Methods

### 2.1. Research Aircraft and Flight Patterns

The aerosol and droplet concentrations used in this study were measured in and around convective clouds with under-wing aerosol and cloud probes mounted on the High Altitude and Long Range Aircraft (HALO) during the ACRIDICON–CHUVA campaign (Wendisch et al., 2016). HALO was equipped with a meteorological sensor system (BAsic HALO Measurement And Sensor System—BAHAMAS) located at the nose of the aircraft (Wendisch et al., 2016). Measurements of air temperature, relative humidity, and vertical wind speed were performed during the flights with uncertainties of about 0.5 K, 5%, and 0.3 m $s^{-1}$, respectively. The description of the corresponding basic principles and uncertainties is available in Mallaun et al. (2015). The HALO flights took place over the Amazon region under various conditions of aerosol concentrations and land cover (e.g., forested and deforested areas) as outlined in Wendisch et al. (2016). Figure 1 shows the flight tracks of cloud profiling maneuvers inside convective clouds used in this study; they were selected based on the availability of aerosol and cloud data and particle hygroscopicity ($\kappa$) (Braga et al., 2021). Furthermore, the analyses were performed for flights in which precipitating and non-precipitating clouds were found and without relevant pollution plumes above cloud bases. The cloud passes used in our study took place in isolated convective clouds with at least 5 km horizontal distance from other clouds. Convective clouds formed in lightly polluted air masses were investigated above the Amazon forest during flights AC09 and AC18. Clouds forming in deforested regions in very polluted (biomass burning) environments were measured during flight AC07.

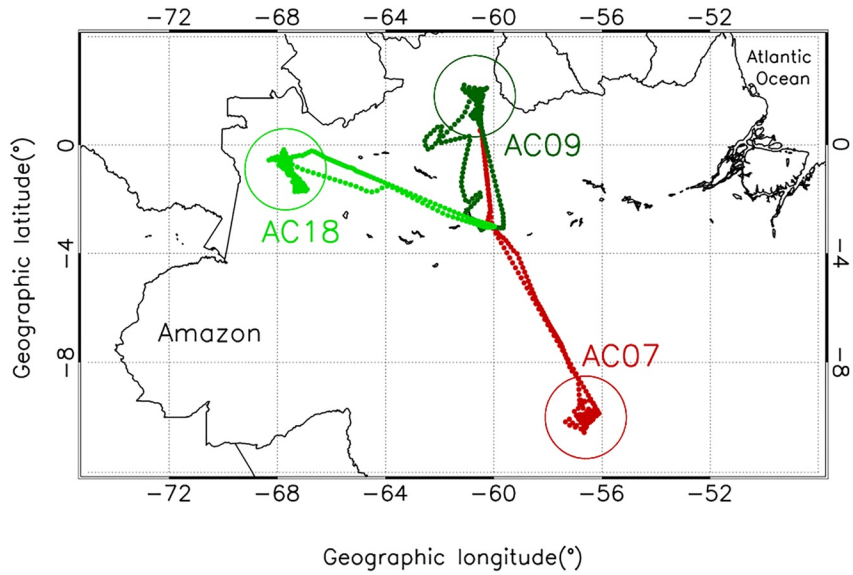


**Figure 1.** Three selected High Altitude and Long Range Aircraft flight tracks during the ACRIDICON–CHUVA campaign that are analyzed in this study. The flight number is indicated by colors. Colored circles indicate the region of convective cloud profiling in each flight. Clouds in lightly polluted conditions were studied during flights AC09 and AC18 over the tropical rain forest (shown in green). Polluted clouds forming in deforested regions were measured during flights AC07 (shown in red). The average total aerosol particle concentrations measured below cloud base during flights AC07, AC09, and AC18 were 2,417, 737, and 809 $cm^{-3}$, respectively (Braga et al., 2021).

### 2.2. Aerosol Particle Measurements

We derived the number concentrations of accumulation-mode aerosol particles ($N_{acc}$) from aerosol size distributions measured with an Ultra-High Sensitivity Aerosol Spectrometer (UHSAS; Droplet Measurement Technologies, Inc., Longmont, CO, USA) (Cai et al., 2008; Moore et al., 2021). The aircraft instrument measured particles in the diameter size range between 92 and 600 nm. The instrument was mounted in an under-wing canister. The sampled air entered the instrument by a forward facing diffusor inlet, and the airflow was reduced by a second inlet to ensure approximately isokinetic sampling conditions. The measured particle diameter is assumed to be close to their dry diameters due to heating effects, which has been justified by Chubb et al. (2016).

The uncertainty in the sizing of UHSAS particle measurement during the ACRIDICON-CHUVA campaign was about 15%. However, for very smoky conditions that contain a lot of black carbon (BC) such values can be higher (an average of about 20% for particles larger than 300 nm) (Howell et al., 2021). However, the data used in our analysis from flights AC07, AC09, and AC18 presented a maximum fraction of absorbing BC aerosols of about 10%, and thus, the undersizing of particles by UHSAS measurements is not an issue for our analysis (see Figure S1 in Supporting Information S1). We also show in Section 3 a case study of UHSAS particle measurements during flight AC19, where the effect of long-range transport of biomass burning aerosols at the lateral boundaries of convective clouds is observed. During this flight, the fraction of BC particles reached values of about 30% (Holanda et al., 2020). This data was not used to describe our conceptual model of aerosol-cloud interactions in the lateral boundaries of convective clouds but rather is shown to illustrate the effect of particles increasing in concentration due to the long-range transport above the cloud bases' heights. Additional information about aerosol measurements is available in the Supporting Information S1.

### 2.3. Cloud Droplet Measurements

Cloud droplet number concentrations and size distributions were measured by a Cloud Combination Probe—Cloud Droplet Probe (CCP-CDP), and by a Cloud and Aerosol Spectrometer with Depolarization (CAS-DPOL) mounted below the wings of HALO (Voigt et al., 2017; Wendisch et al., 2016). Precipitating particle number concentrations and size distributions were measured by the Cloud Imaging Probe (CIPgs) mounted on the CCP. The information from CCP–CIPgs were used in this study to identify cloud with raindrops. From data of CAS-DPOL, CCP-CDP

and CCP-CIPgs, hydrometeor particles ranging from 3 to 960 μm in diameter ($d$) were measured within clouds. Additional details about the cloud probe measurement characteristics during ACRIDICON-CHUVA campaign are described in Wendisch et al. (2016), Weigel et al. (2016), Braga et al. (2017a), Jäkel et al. (2017), Cecchini et al. (2017), Braga et al. (2017b) and in the Supporting Information S1.

### 2.4. Data Analysis

#### 2.4.1. Comparison of $N_{acc}$ and $N_d$

The UHSAS measurements of $N_{acc}$ at the lateral boundaries of convective clouds (up to ~500 m away from the cloud edges) were analyzed as a function of the measurements of $N_d$ from CAS-DPOL and CCP-CDP at cloud base and above cloud base. Data from UHSAS out of clouds (i.e., when $N_d = 0$) were used in the analysis. Only cloud passes with at least 3 s of consecutive measurements (i.e., with lengths larger than ~200 m) of $N_d > 20$ cm$^{-3}$ along the aircraft traverse were taken into account. This criterion was applied to avoid cloud passes well mixed with subsaturated environment air (relative humidity <100%) and counts of haze particles, typically found at cloud edges and dissipating convective clouds. Furthermore, the precipitation water content (PWC) is calculated to detect cloud passes with raindrops. The following calculation were conducted during our analysis:

$$N_d = \int_{1.5\mu m}^{25\mu m} N(r)dr \quad (1)$$

$$N_{acc} = \int_{0.1\mu m}^{0.6\mu m} N(r)dr \quad (2)$$

$$PWC = \frac{4\pi}{3}\rho \int_{25\mu m}^{480\mu m} r^3\, N(r)dr \quad (3)$$

where $N$ is the particle number concentration (in cm$^{-3}$), $\rho$ is the particle density (in g cm$^{-3}$), and $r$ is the particle radius ($\mu$m). Braga et al. (2017a) showed that cloud and rain liquid water drops dominated for air temperatures $T > -9$°C over the Amazon. For $T \leq -9$°C, ice initiation was found. Here, we focus our analysis on particles in the liquid phase, and thus, only cloud particles measured at $T > -9$°C are used. Therefore, the density of liquid water (1 g cm$^{-3}$) is assumed in our calculations.

#### 2.4.2. Calculation of $S_w$ Within Cloud

The retrieval of $S_w$ within cloud is based on the calculation of the critical supersaturation ($S_c$) for a dry aerosol particle, according to Köhler theory (Köhler, 1936). Here, the particle hygroscopicity parameter ($\kappa$) is used to represent the solute composition of the dry aerosol particle (Petters & Kreidenweis, 2007). In addition, we assume the surface tension of water (72 mN m$^{-1}$) for particles and $T$ measured concurrently with $N_{acc}$ to calculate $S_c$. The retrieved $S_c$ is assumed as the maximum $S_w$ within the convective cloud. The relationship between droplet activation efficiency and $S_w$ is estimated for cloud base altitude and above cloud base. This approach is typically used in calculations of the CCN efficiency, given by the ratio between the number concentrations of CCN at a given $S_w$ ($N_{CCN}(S_w)$) and of condensation nuclei ($N_{CN}$) (Pöhlker et al., 2018). From the calculated CCN efficiency, the $\kappa$ of the corresponding aerosol particles can be estimated, assuming an initial particle size distribution (PSDs). Here, we follow a similar approach for real clouds, in which different microphysical processes also take place (e.g., coalescence of droplets, turbulent mixing etc.). The droplet activation efficiency is calculated from the maximum $N_d$ measured during the cloud passes and the maximum $N_{acc}$ measured up to ~500 m away from the cloud edges. This approach is based on the assumption that during the cloud mixing process the maximum $N_d$ within cloud is resulting from the maximum $N_{acc}$ available around clouds. Additional information about $S_w$ retrieval within cloud is available in the Supporting Information S1.

Overall, 128 cloud passes were used in our analysis (~95% of cloud passes available). The lack of information about Aitken mode particle sizes prevented us to extend our analysis for cases in which the maximum $N_d$ were larger than the maximum $N_{acc}$ around the clouds. Nevertheless, as these cloud passes were in minor number (~5% of cloud passes) we assumed that the measured $N_{acc}$ with the UHSAS was a reasonable estimation of CCN concentrations around convective clouds. Assuming $\kappa$ values of 0.1–0.2 and the lower cutoff of 100 nm for $N_{acc}$, the UHSAS measurements of $N_{acc}$ are a proxy for the CCN concentrations at 0.37%-0.26%, respectively.

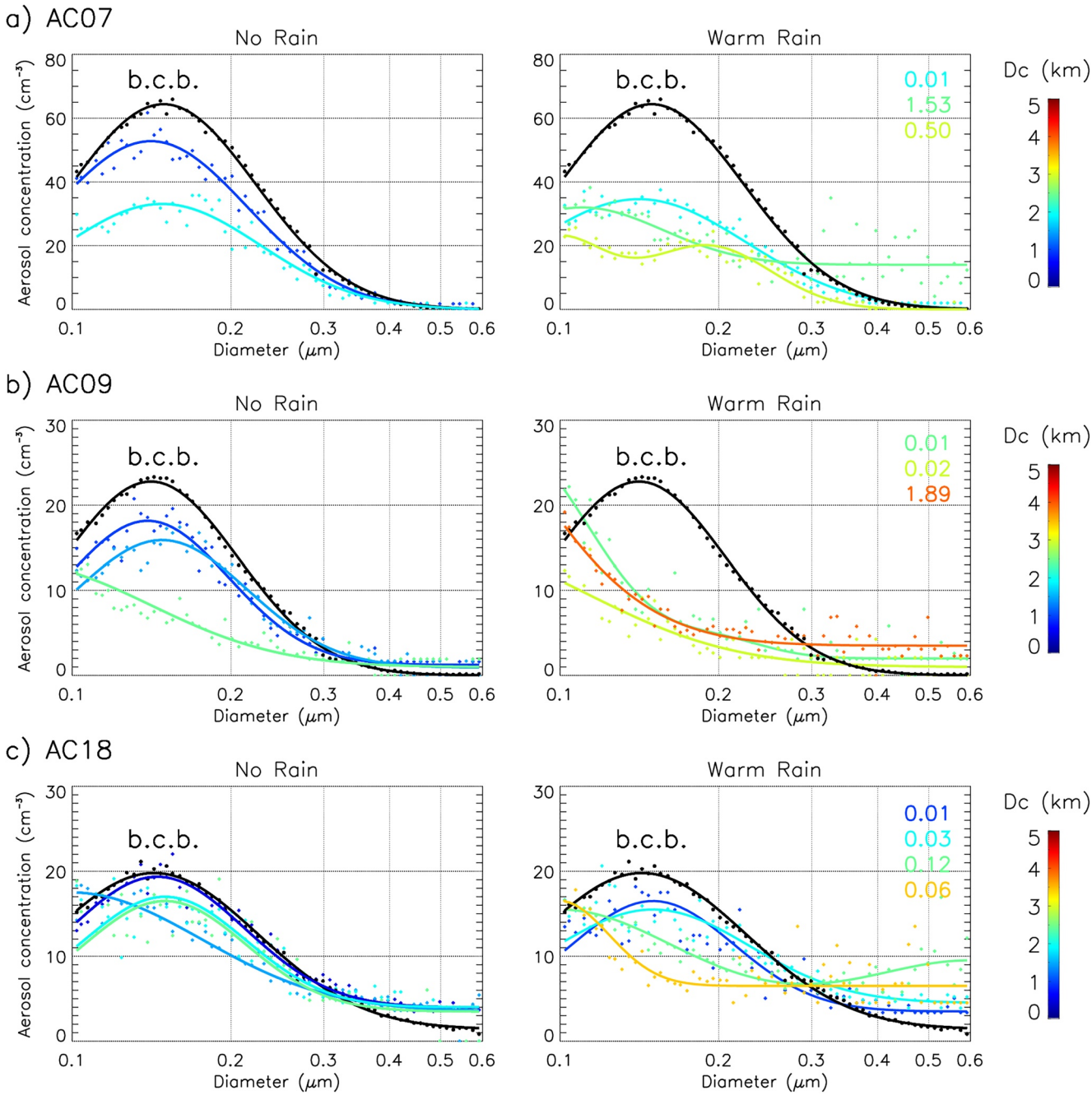


**Figure 2.** (a) Average number concentration of aerosol particles as a function of particle diameter measured by Ultra-High Sensitivity Aerosol Spectrometer below cloud base (b.c.b.; in black dots) during flight AC07 and at the lateral boundaries of non-precipitating (left) and precipitating (right) convective clouds at different heights above cloud base level ($D_c$). $D_c$ is labeled by the color bar on the right. Solid lines indicate the logarithm fit of averaged measurements. Measurements at the lateral boundaries of clouds were made between 100 and 500 m away from the cloud edges. The maximum precipitation water content (in g $m^{-3}$) during the cloud passes is shown on the upper-right corner of the right panels. (b and c) Similar for flights AC09 and AC18, respectively.

## 3. Results

We investigated the effect of cloud processing on CCN concentrations around clouds based on PSDs measured below and above the bases of convective clouds. Figure 2 shows the comparison between the average PSDs measured below and at the lateral boundaries of non-precipitating and precipitating ice-free convective clouds. For non-precipitating clouds, Figures 2a–2c show a decrease in the concentration of the smaller particle sizes compared to measurements below cloud bases, which is hypothesized to be caused by aerosol cloud processing.

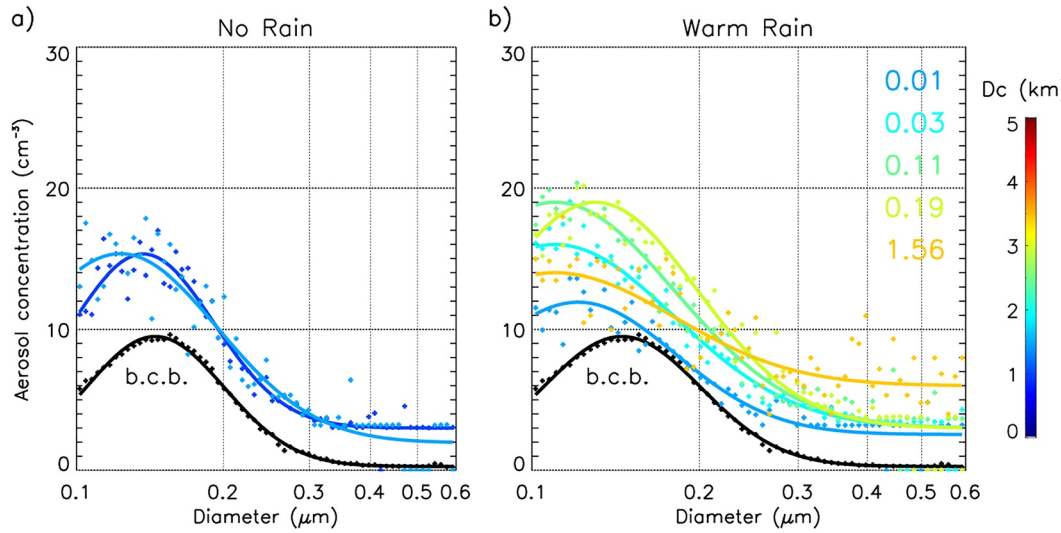


**Figure 3.** Similar to Figure 2 for measurements above the Atlantic Ocean performed during flight AC19. (a) At the lateral boundaries of non-precipitating and (b) precipitating convective clouds at different heights above cloud base level ($D_c$).

Out of clouds, larger aerosol particles should decrease faster with height if no cloud processing is involved. However, Figure 2 shows smaller sizes reducing more quickly with height. This is the fingerprint of cloud processing in the air out of inuds.

A fewer concentration of large aerosol particles ($d > 0.3$ μm) is observed above the forested region (flights AC09 athe nd AC18) compared to above the deforestation arc, probably due to the more significant fraction of natural organic aerosols. Such larger particles are also observed in PSDs out of clouds at longer horizontal distances (see Figure S3 in Supporting Information S1).

In precipitating clouds, an increase of larger particles at the expense of smaller particles is observed for different heights above cloud base level ($D_c$). The increased concentration of larger particles is likely a result of cloud processing and is more evident at greater heights, where collision and coalescence processes (PWC) are more intense. These results highlight that the coagulation processes within convective clouds play a crucial role for the sizes of CCN particles resulting from detrained cloud volumes. For clouds with warm rain, an even more pronounced relative increase in concentration of larger particles at the expense of small particles is observed at the lateral boundaries of convective clouds than for clouds without precipitation.

Similar changes in PSDs and concentrations around convective clouds were not observed when long-range transport of aerosol particle was dominant. Figure 3 shows a comparison between the average PSDs measured during flight AC19 below and at the lateral boundaries of non-precipitating and precipitating convective clouds. The measurements took place above the Atlantic Ocean, where warm convective clouds were present. During flight AC19 an increase of particles concentration with height due to long-range transport of biomass burning particles in elevated haze layers was observed (Holanda et al., 2020). The additional CCN particles at higher altitudes was also observed in UHSAS measurements, as shown in Figure 3. This figure shows that CCN concentrations below cloud bases were much smaller than those measured at the lateral boundaries of convective clouds. The increase in concentration was measured for particles across the whole range of sizes detected by the UHSAS, suggesting that in this case, the mixing at the cloud edges resulted in a transport of particles into the cloud, rather than the cloud being a source of particles to the surrounding atmosphere as in the previously discussed cases.

In order to investigate the effect of cloud droplet evaporation on CCN concentrations around convective clouds, we have also analyzed the droplet activation efficiency as a function of $S_w$ at different $D_c$. The method is described in th,e Supporting Information S1. Figure 4 shows the measured droplet activation efficiency and $S_w$ at and above cloud base in convective clouds. Figure 4a shows that the relationship between droplet activation efficiency and $S_w$ for measurements at cloud base can be well expressed by an single-error function (erf) fit parametrization ($R^2 \sim 0.96$). Similar tight relationship are found in CCN counters between CCN efficiency and $S_w$, where the environmental $S_w$ is controlled (Dusek et al., 2006). Remarkably, measurements for heights 200 m above cloud

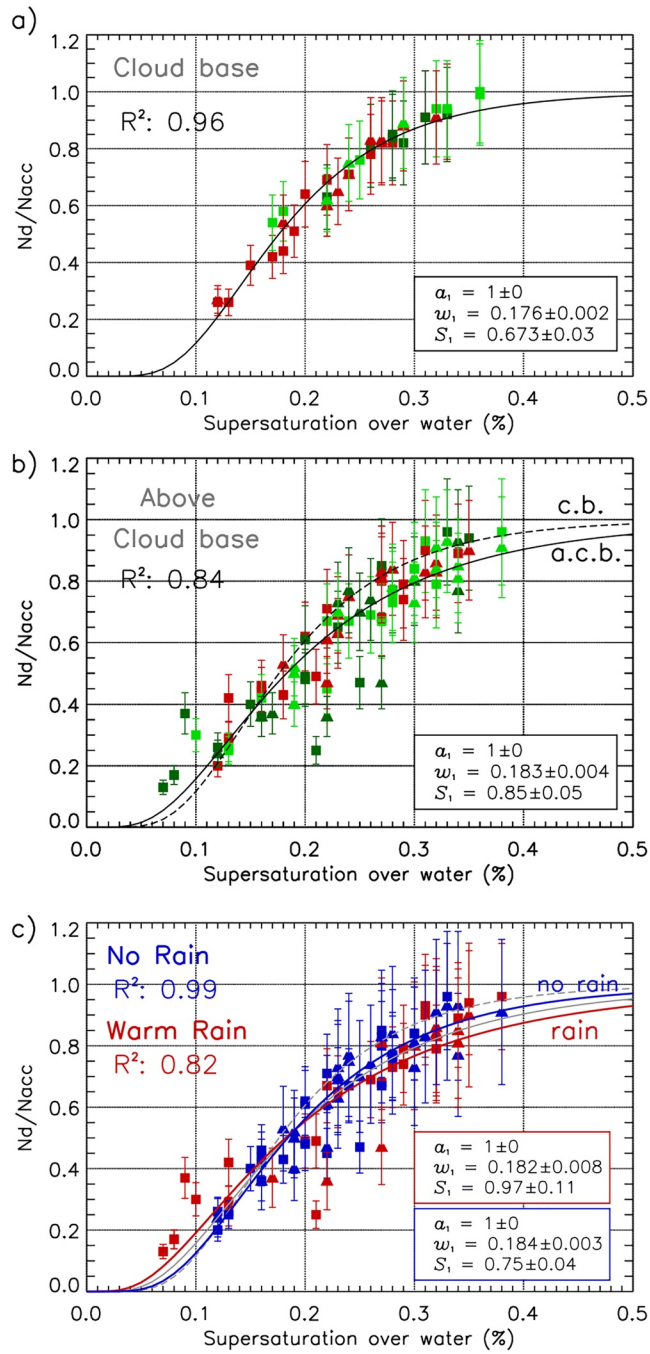


**Figure 4.** (a) Droplet activation efficiency ($N_d/N_{acc}$) as a function of $S_w$ for cloud base measurements over different regions (Forested (AC09)—light green; Forested (AC18)—dark green and Deforested (AC07)—red). The droplet activation efficiency calculated with Cloud Combination Probe—Cloud Droplet Probe (CCP-CDP) and Cloud and Aerosol Spectrometer with Depolarization (CAS-DPOL) measurements are indicated by squares and triangles, respectively. The error bars indicate the measurement uncertainties of droplet activation efficiencies calculated with CCP-CDP and CAS-DPOL (~18% and ~26%, respectively). The black line indicates the erf fit for droplet activation efficiency as a function of $S_w$ (the parameters of the erf fit from Equation S1 in Supporting Information S1 are indicated in the black box). The $R^2$ from this fit function is 0.96. (b) Similar as (a) for measurements at heights 200 m above cloud base. The dashed line indicates the erf fit for cloud base measurements from panel (4a). (c) Similar as (b) for measurements at heights above cloud base with precipitation (PWC > 0.01 g $m^{-3}$) in red and non-precipitating cloud passes (in blue). The solid red (blue) line indicates the erf fit for measurements with (without) precipitation above cloud base and the dashed and solid gray lines indicate the erf fit shown in panel (4b).

base shown in Figure 4b indicate that the relationship between droplet activation efficiency and $S_w$ still has a high correlation, but with smaller agreement ($R^2 \sim 0.84$). The figure shows that the values of droplet activation efficiencies are shifted down for cloud passes above cloud base in comparison with cloud base measurements. These results suggest that cloud processing above cloud base decorrelates the relationship between droplet activation efficiency and $S_w$. Figure 4c shows that for non-precipitating clouds the relationship between droplet activation efficiency and $S_w$ has a high correlation ($R^2 \sim 0.99$), while for precipitating clouds the $R^2$ of the erf fit considerably decreases ($R^2 \sim 0.82$).

For precipitating clouds a relative decrease in $N_d$ is expected due to the coalescence processes. Our analysis show that precipitation would decrease the droplet activation efficiency. However, the opposite effect is expected out of clouds since the size of detrained particles are larger than below cloud base. Above cloud base, chemical cloud processing may also shift the particle hygroscopicity ($\kappa$) away from the value assumed ($\kappa = 0.1$) when estimating $S_w$ (Ervens et al., 2018; Rissler et al., 2006). For accumulation mode particles we have estimated values slightly larger for some cloud passes above the Amazon Basin ($\kappa \sim 0.15 - 0.2$). The practical effect of changing $\kappa$ will lead to a shift to smaller values on the calculated $S_w$ but with no change of the correlation between droplet activation efficiency and $S_w$ (see Figure S4 in Supporting Information S1 for results assuming $\kappa = 0.2$). Furthermore, we have shown that for this range of $\kappa$ values the sensitivity of droplet concentration to $\kappa$ is low for accumulation mode particles (Pöhlker et al., 2021). The values of $S_w$ estimated in our analysis are in the same range of those measured with CCN counter in the Amazon during the dry season (Pöhlker et al., 2018). Additional analysis with CCN measurements available onboard the HALO aircraft were not possible since the particle's inlets of UHSAS and CCN counters were different. In such conditions, the number concentration of particles may be underestimated by one of the instruments, and thus, leading to additional uncertainties on calculating particle's hygroscopicity from these measured data.

## 4. Discussion

The effect of cloud droplet evaporation on aerosol concentration around non-precipitating convective clouds was previously observed by Zhu et al. (2015). Based on satellite measurements, these authors observed an enhancement in the aerosol optical depth around convective clouds due to aerosol upward transport and detrainment from the clouds below the level of rain initiation. Our results of droplet activation efficiencies from measurements at cloud base heights and above cloud base suggest that the $N_{acc}$ around the ice-free convective clouds are dominated by the evaporation of detrained cloud droplets in absence of relevant amount of long-range transport of CCN particles. For clouds with warm rain, $N_d$ decreases due to the coalescence processes and its concentration may not dominate the $N_{acc}$ at the lateral boundaries of the clouds. This leads to an unrealistic decrease in the droplet activation efficiency since larger particles are detrained from clouds.

Here, we show for the first time that the expected relationships between aerosol particle number concentration, critical supersaturation and $N_d$ is found for measurements above the cloud bases of convective clouds. These results were found from airborne measurements under different thermodynamic and pollution conditions over the Amazon basin. The tight relationship between droplet activation efficiency and $S_w$ (similar as found with data measured with CCN counters) suggests that based on measurements of $N_d$, $N_{acc}$, and particle hygroscopicity one may estimate $S_w$ within non-precipitating convective clouds. Furthermore, the fact that there is a high correlation between $N_d$ and $N_{acc}$ at the lateral boundaries of non-precipitating convective clouds supports the hypothesis that residual particles from evaporation of droplets dominate CCN concentrations around them.

Accounting for CCN concentrations and sizes available through the evaporation of cloud droplets and raindrops is extremely complicated and a crucial challenge for cloud modeling purposes (Khain et al., 2015). Important uncertainties result from the lack of accurate information about the chemical composition and soluble mass of evaporated droplets. Our findings in this study suggest that during the dry season in the Amazon basin accumulation mode particles measured at the lateral boundaries of non-precipitating clouds have similar hygroscopicity ($\kappa$) and sizes to those found below cloud bases. Above the height of rain initiation these CCN particles are relatively larger than those found below cloud bases, and thus, particle hygroscopicity might not be the same as found below cloud bases due to cloud processing mechanisms.

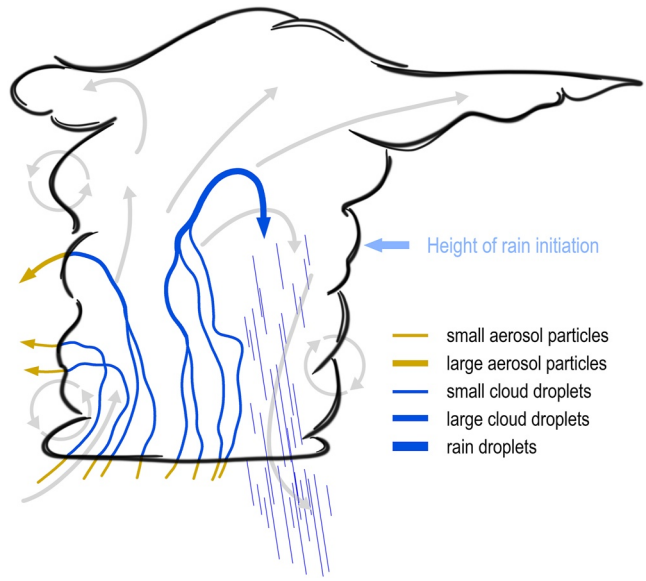


**Figure 5.** Schematic description of particles path within and at the lateral boundaries of growing convective cumulus. The gray arrows indicate the overall air flow pattern within cloud, and colored arrows (labeled on the right) are the particle tracks from below cloud base up to where they exit the cloud volume or coalesce into raindrops. Cloud condensation nuclei (CCN) particles ingested from below cloud base are activated into cloud droplets; when these evaporate at the lateral boundaries and above cloud base, they release the CCN again. When drops coalesce and then leave the cloud, only one CCN is formed back. When cloud droplets coalesce and precipitate, the CCN that produced the rain drops do not detrain from the cloud but are deposited to the ground. The detrainment of cloudy volumes into the surrounding clear air lead to a decrease of the drop concentration while increasing the CCN concentration around the cloud.

Figure 5 summarizes our findings on the cloud particles' path within and at the lateral boundaries of growing convective cumulus schematically. At cloud bases the turbulent mixing leads to the entrainment of CCN particles from lower levels and their activation into cloud droplets. CCN particles ingested from below cloud bases may evaporate at the lateral boundaries and above cloud base becoming (cloud processed) CCN again. When collision and coalescence processes are relevant, smaller droplets are removed, which diminishes the population of detrained droplets evaporated outside clouds and thus CCN concentrations. As a consequence, however, larger CCN particles are resulting from detrained droplets of precipitating clouds. This conceptual model emphasizes that non-precipitating convective clouds are dominant in production of CCN particles at their lateral boundaries whereas the CCN concentrations in air detrained from precipitating clouds are depleted due to scavenging. When long-range transport of CCN particles is relevant at higher altitudes, the additional CCN particles overwhelm the effect of convective clouds in the release of CCN particles at the lateral boundaries of clouds. Our results suggest that the mixing of long-range transported particles at the cloud edges results in a transport of particles into the cloud, rather than the cloud being a source of particles to the surrounding atmosphere.

This study demonstrated the importance of the details of aerosol processing and its partition to detrainment and scavenging. A future study with measurements from a counterflow virtual impactor (Noone et al., 1988; Twohy et al., 1997) and analysis of single particle composition would advance the general insights of this study to better quantification of the effects.

## Data Availability Statement

The data used in this study can be found at https://halo-db.pa.op.dlr.de/mission/5 (last access: 1 May 2022, Deutsches Zentrum für Luft- und Raumfahrt, 2014).

**Acknowledgments**
We thank the ACRIDICON-CHUVA team. The ACRIDICON-CHUVA campaign was supported by the Max Planck Society (MPG), the German Science Foundation (DFG Priority Program SPP 1294), the German Aerospace Center (DLR), and a wide range of other institutional partners. CV thanks funding by DFG within co no VO 1504/6-1. Open access publishing facilitated by Southern Cross University, as part of the Wiley - Southern Cross University agreement via the Council of Australian University Librarians.

## References

Andreae, M. O., Rosenfeld, D., Artaxo, P., Costa, A. A., Frank, G. P., Longo, K. M., & Silva-Dias, M. A. F. (2004). Smoking rain clouds over the Amazon. *Science*, *303*(5662), 1337–1342. https://doi.org/10.1126/science.1092779

Beals, M. J., Fugal, J. P., Shaw, R. A., Lu, J., Spuler, S. M., & Stith, J. L. (2015). Holographic measurements of inhomogeneous cloud mixing at the centimeter scale. *Science*, *350*(6256), 87–90. https://doi.org/10.1126/science.aab0751

Bera, S., Pandithurai, G., & Prabha, T. (2016). Entrainment and droplet spectral characteristics in convective clouds during transition to monsoon. *Atmospheric Science Letters*, *17*(4), 286–293. https://doi.org/10.1002/asl.657

Braga, R. C., Ervens, B., Rosenfeld, D., Andreae, M. O., Förster, J.-D., Fütterer, D., et al. (2021). Cloud droplet formation at the base of tropical convective clouds: Closure between modeling and measurement results of ACRIDICON–CHUVA. *Atmospheric Chemistry and Physics*, *21*(23), 17513–17528. https://doi.org/10.5194/acp-21-17513-2021

Braga, R. C., Rosenfeld, D., Weigel, R., Jurkat, T., Andreae, M. O., Wendisch, M., et al. (2017a). Further evidence for CCN aerosol concentrations determining the height of warm rain and ice initiation in convective clouds over the Amazon basin. *Atmospheric Chemistry and Physics*, *17*(23), 14433–14456. https://doi.org/10.5194/acp-17-14433-2017

Braga, R. C., Rosenfeld, D., Weigel, R., Jurkat, T., Andreae, M. O., Wendisch, M., et al. (2017b). Comparing parameterized versus measured microphysical properties of tropical convective cloud bases during the ACRIDICON-CHUVA campaign. *Atmospheric Chemistry and Physics*, *17*(12), 7365–7386. https://doi.org/10.5194/acp-2016-872

Burnet, F., & Brenguier, J.-L. (2007). Observational study of the entrainment-mixing process in warm convective clouds. *Journal of the Atmospheric Sciences*, *64*(6), 1995–2011. https://doi.org/10.1175/JAS3928.1

Cai, Y., Montague, D. C., Mooiweer-Bryan, W., & Deshler, T. (2008). Performance characteristics of the ultra high sensitivity aerosol spectrometer for particles between 55 and 800 nm: Laboratory and field studies. *Journal of Aerosol Science*, *39*(9), 759–769. https://doi.org/10.1016/j.jaerosci.2008.04.007

Cecchini, M. A., Machado, L. A. T., Andreae, M. O., Martin, S. T., Albrecht, R. I., Artaxo, P., et al. (2017). Sensitivities of Amazonian clouds to aerosols and updraft speed. *Atmospheric Chemistry and Physics*, *17*(16), 10037–10050. https://doi.org/10.5194/acp-17-10037-2017

Chubb, T., Huang, Y., Jensen, J., Campos, T., Siems, S., & Manton, M. (2016). Observations of high droplet number concentrations in southern ocean boundary layer clouds. *Atmospheric Chemistry and Physics*, *16*(2), 971–987. https://doi.org/10.5194/acp-16-971-2016

Dusek, U., Frank, G. P., Hildebrandt, L., Curtius, J., Schneider, J., Walter, S., et al. (2006). Size matters more than chemistry for cloud-nucleating ability of aerosol particles. *Science*, *312*(5778), 1375–1378. https://doi.org/10.1126/science.1125261

Ervens, B., Sorooshian, A., Aldhaif, A. M., Shingler, T., Crosbie, E., Ziemba, L., et al. (2018). Is there an aerosol signature of chemical cloud processing? *Atmospheric Chemistry and Physics*, *18*(21), 16099–16119. https://doi.org/10.5194/acp-18-16099-2018

Fan, J., Rosenfeld, D., Zhang, Y., Giangrande, S. E., Li, Z., Machado, L. A. T., et al. (2018). Substantial convection and precipitation enhancements by ultrafine aerosol particles. *Science*, *359*(6374), 411–418. https://doi.org/10.1126/science.aan8461

Freud, E., Rosenfeld, D., Axisa, D., & Kulkarni, J. (2011). Resolving both entrainment-mixing and number of activated CCN in deep convective clouds. *Atmospheric Chemistry and Physics*, *11*, 9673–9703. https://doi.org/10.5194/acpd-11-9673-2011

Gerber, H., Frick, G., Jensen, J., Hudson, J., & Gerber (2008). Entrainment, mixing, and microphysics in trade-wind cumulus. *Journal of the Meteorological Society of Japan*, *86*, 87–106. https://doi.org/10.2151/jmsj.86A.87

Haarig, M., Walser, A., Ansmann, A., Dollner, M., Althausen, D., Sauer, D., et al. (2019). Profiles of cloud condensation nuclei, dust mass concentration, and ice-nucleating-particle-relevant aerosol properties in the Saharan air layer over Barbados from polarization Lidar and airborne in situ measurements. *Atmospheric Chemistry and Physics*, *19*(22), 13773–13788. https://doi.org/10.5194/acp-19-13773-2019

Holanda, B. A., Pöhlker, M. L., Walter, D., Saturno, J., Sörgel, M., Ditas, J., et al. (2020). Influx of african biomass burning aerosol during the Amazonian dry season through layered transatlantic transport of black carbon-rich smoke. *Atmospheric Chemistry and Physics*, *20*(8), 4757–4785. https://doi.org/10.5194/acp-20-4757-2020

Howell, S. G., Freitag, S., Dobracki, A., Smirnow, N., & Sedlacek, A. J., III. (2021). Undersizing of aged African biomass burning aerosol by an ultra-high-sensitivity aerosol spectrometer. *Atmospheric Measurement Techniques*, *14*(11), 7381–7404. https://doi.org/10.5194/amt-14-7381-2021

Jäkel, E., Wendisch, M., Krisna, T. C., Ewald, F., Kölling, T., Jurkat, T., et al. (2017). Vertical distribution of the particle phase in tropical deep convective clouds as derived from cloud-side reflected solar radiation measurements. *Atmospheric Chemistry and Physics*, *17*(14), 9049–9066. https://doi.org/10.5194/acp-17-9049-2017

Khain, A. P., Beheng, K. D., Heymsfield, A., Korolev, A., Krichak, S. O., Levin, Z., et al. (2015). Representation of microphysical processes in cloud-resolving models: Spectral (bin) microphysics versus bulk parameterization. *Reviews of Geophysics*, *53*(2), 247–322. https://doi.org/10.1002/2014RG000468

Khain, A. P., & Pinsky, M. (2018). *Physical processes in clouds and cloud modeling*. (p. 278). Cambridge University Press.

Köhler, H. (1936). The nucleus in and the growth of hygroscopic droplets. *Transactions of the Faraday Society*, *32*(0), 1152–1161. https://doi.org/10.1039/tf9363201152

Kokhanovsky, A. (2004). Optical properties of terrestrial clouds. *Earth-Science Reviews*, *64*(3), 189–241. https://doi.org/10.1016/S0012-8252(03)00042-4

Mallaun, C., Giez, A., & Baumann, R. (2015). Calibration of 3-D wind measurements on a single-engine research aircraft. *Atmospheric Measurement Techniques*, *8*(8), 3177–3196. https://doi.org/10.5194/amt-8-3177-2015

Mamouri, R.-E., & Ansmann, A. (2016). Potential of polarization Lidar to provide profiles of CCN- and INP-relevant aerosol parameters. *Atmospheric Chemistry and Physics*, *16*(9), 5905–5931. https://doi.org/10.5194/acp-16-5905-2016

Moore, R. H., Wiggins, E. B., Ahern, A. T., Zimmerman, S., Montgomery, L., Campuzano Jost, P., et al. (2021). Sizing response of the ultra-high sensitivity aerosol size spectrometer (UHSAS) and laser aerosol spectrometer (LAS) to changes in submicron aerosol composition and refractive index. *Atmospheric Measurement Techniques Discussions*, 1–36. https://doi.org/10.5194/amt-2021-21

Noone, K. J., Ogren, J. A., Heintzenberg, J., Charlson, R. J., & Covert, D. S. (1988). Design and calibration of a counterflow virtual impactor for sampling of atmospheric fog and cloud droplets. *Aerosol Science and Technology*, *8*(3), 235–244. https://doi.org/10.1080/02786828808959186

Petters, M. D., & Kreidenweis, S. M. (2007). A single parameter representation of hygroscopic growth and cloud\ncondensation nucleus activity. *Atmospheric Chemistry and Physics*, *7*(8), 1961–1971. https://doi.org/10.5194/acp-7-1961-2007

Pöhlker, M. L., Ditas, F., Saturno, J., Klimach, T., Hrabě de Angelis, I., Araùjo, A. C., et al. (2018). Long-term observations of cloud condensation nuclei over the amazon rain forest—Part 2: Variability and characteristics of biomass burning, long-range transport, and pristine rain forest aerosols. *Atmospheric Chemistry and Physics*, *18*(14), 10289–10331. https://doi.org/10.5194/acp-18-10289-2018

Pöhlker, M. L., Zhang, M., Campos Braga, R., Krüger, O. O., Pöschl, U., & Ervens, B. (2021). Aitken mode particles as CCN in aerosol- and updraft-sensitive regimes of cloud droplet formation. *Atmospheric Chemistry and Physics*, *21*(15), 11723–11740. https://doi.org/10.5194/acp-21-11723-2021

Pruppacher, H., & Klett, J. D. (1997). *Microphysics of clouds and precipitation* (2nd ed., pp. 493–497). Kluwer Academic Publishers.

Rissler, J., Vestin, A., Swietlicki, E., Fisch, G., Zhou, J., Artaxo, P., & Andreae, M. O. (2006). Size distribution and hygroscopic properties of aerosol particles from dry-season biomass burning in Amazonia. *Atmospheric Chemistry and Physics*, *6*(2), 471–491. https://doi.org/10.5194/acp-6-471-2006

Rogers, R., & Yau, M. (1989). *A short course in cloud physics*. (p. 94). Elsevier Science & Technology Books.

Rosenfeld, D., Lohmann, U., Raga, G. B., O'Dowd, C. D., Kulmala, M., Fuzzi, S., et al. (2008). Flood or drought: How do aerosols affect precipitation? *Science*, *321*(5894), 1309–1313. https://doi.org/10.1126/science.1160606

Twohy, C. H., Schanot, A. J., & Cooper, W. A. (1997). Measurement of condensed water content in liquid and ice clouds using an airborne counterflow virtual impactor. *Journal of Atmospheric and Oceanic Technology*, *14*(1), 197–202. https://doi.org/10.1175/1520-0426(1997)014<0197:mocwci>2.0.co;2

Twomey, S. (1974). Pollution and the planetary albedo. *Atmospheric Environment*, *8*(12), 1251–1256. https://doi.org/10.1016/0004-6981(74)90004-3

Voigt, C., Schumann, U., Minikin, A., Abdelmonem, A., Afchine, A., Borrmann, S., et al. (2017). Ml-cirrus: The airborne experiment on natural cirrus and contrail cirrus with the high-altitude long-range research aircraft halo. *Bulletin of the American Meteorological Society*, *98*(2), 271–288. https://doi.org/10.1175/BAMS-D-15-00213.1

Weigel, R., Spichtinger, P., Mahnke, C., Klingebiel, M., Afchine, A., Petzold, A., et al. (2016). Thermodynamic correction of particle concentrations measured by underwing probes on fast-flying aircraft. *Atmospheric Measurement Techniques*, *9*(10), 5135–5162. https://doi.org/10.5194/amt-9-5135-2016

Wendisch, M., Poschl, U., Andreae, M. O., MacHado, L. A. T., Albrecht, R., Schlager, H., et al. (2016). ACRIDICON-CHUVA campaign: Studying tropical deep convective clouds and precipitation over Amazonia using the New German research aircraft HALO. *Bulletin of the American Meteorological Society*, *97*(10), 1885–1908. https://doi.org/10.1175/BAMS-D-14-00255.1

Zhu, Y., Rosenfeld, D., Yu, X., & Li, Z. (2015). Separating aerosol microphysical effects and satellite measurement artifacts of the relationships between warm rain onset height and aerosol optical depth. *Journal of Geophysical Research: Atmospheres*, *120*(15), 7726–7736. https://doi.org/10.1002/2015JD023547